Users First: User-Centric Cluster Formation for Interference-Mitigation in Visible-Light Networks

Xuan Li[1], Fan Jin[1], Rong Zhang[1], Jiaheng Wang[2], Zhengyuan Xu[3], Lajos Hanzo[1]
[1] University of Southampton, UK, xl26g12,fj1g10,rz,lh@ecs.soton.ac.uk
[2] Southeast University, China, jhwang@seu.edu.cn
[3] University of Science and Technology of China, China, xuzy@ustc.edu.cn

***Abstract*—Visible Light Communication (VLC) combined with advanced illumination may be expected to become an integral part of next generation heterogeneous networks. In order to mitigate the performance degradation imposed by the Inter-Cell-Interference (ICI), a User-Centric (UC) cluster formation technique employing Vectored Transmission (VT) is proposed for the VLC down-link system, where multiple users may be simultaneously supported by multiple Access Points (APs). In contrast to the traditional Network-Centric (NC) design, the UC-VT cluster formation is dynamically constructed and adjusted, rather than remaining static. Furthermore, we consider the critical issue of Multi-User Scheduling (MUS) relying on maximizing the 'sum utility' of this system, which leads to a joint cluster formation and MUS problem. In order to find a practical solution, the original problem is reformulated as a Maximum Weighted Matching (MWM) problem relying on a user-AP distance-based weight and then a low-complexity greedy algorithm is proposed, which offers a suboptimal yet compelling solution operating close to the optimal value found by the potentially excessive-complexity exhaustive search. Our simulation results demonstrate that the proposed greedy MUS algorithm combined with the UC-VT cluster formation is capable of providing an average user throughput of about 90% of the optimal throughput, which is about three times the throughput provided by the traditional cellular design in some of the scenarios considered.**

***Index Terms*—Visible light communication, user-centric cluster formation, multi-user scheduling, maximum weighted matching.**

I. Introduction

Owing to its huge unlicensed bandwidth, high data rate potential, energy-efficient illumination etc., the research of Visible Light Communication (VLC) intensified during the past decade or so [1]. As a complementary extension of classic radio frequency communications, extensive investigations have been dedicated to the point-to-point transmission and reception techniques in VLC networks [2]–[10], as also indicated by the IEEE 802.15.7 standard ratified for short-range visible light wireless communication [11]. Apart from their multi-fold advantages, naturally, VLC systems also exhibit several potential drawbacks, such as reduced performance in non-line-of-sight scenarios, lack of native up-link support, a confined coverage compared to cellular radio frequency networks etc.

The financial support of the RC-UK under the auspices of the UK-India ATC in Wireless Communications, of the Chinese Scholarship Council as well as of the European Research Council's Advanced Fellow Grant is gratefully acknowledged. J. Wang is supported in part by the 973 Program of China (2013CB336600), the NSFC (61201174), the NSF of Jiangsu (BK2012325), and the Fundamental Research Funds for the Central Universities.

Amongst all the design challenges, the performance degradation imposed by Inter-Cell Interference (ICI) at the cell edge may lead to dramatic reduction of the Quality of Service (QoS) in a VLC down-link system. As a result, careful VLC cell formation becomes crucial, since it is the salient design stage of the entire system design cycle. Traditional designs conceived for VLC cells operating both with and without Frequency Reuse (FR) or fractional frequency reuse planning, have been studied in [12]–[14], where each optical Access Point (AP) illuminates a small confined cell. As a further advance, a multi-AP joint transmission scheme relying on Combined Transmission (CT) and Vectored Transmission (VT) [1] were also investigated in [12]. In contrast to the above-mentioned Network-Centric (NC) design philosophy, a novel User-Centric (UC) cell formation regime was proposed in [15]–[17], where amorphous user-specific multi-AP cells are constructed for jointly transmitting data to a single User Equipment (UE) [2] by employing CT, which we referred to as UC-CT. By definition, UC design is different from the NC design, where the network configuration is fixed, regardless of the tele-traffic. In order to further improve the achievable bandwidth efficiency of the previously proposed UC-CT and to allow each multi-AP cell simultaneously serve multiple UEs as discussed in [12], we propose the *UC-VT-based* cluster formation principle in this paper. UC-VT cluster formation may be defined as forming the UC-VT clusters, where each UC-VT cluster is served by a set of VLC APs, which simultaneously serve multiple UEs by employing VT. More explicitly, a UC-VT cluster includes a set of APs and UEs as well as the transmission links between them. Note that the previously proposed UC-CT-based cell formation of [15]–[17] may be regarded as a special case of our UC-VT-based cluster formation, when only a single UE resides within the coverage of the UC-VT cluster.

When multiple UEs are present in a VLC network, efficient resource allocation and Multi-User Scheduling (MUS) constitutes one of the salient problems, which in fact affects

[1] In [12], relying on CT, each individual VLC AP of a multi-AP cell conveyed the same information on the same visible carrier frequency in their overlapping areas and served a single user at a time. In order to eliminate the bandwidth efficiency reduction imposed by CT, Zero-Forcing (ZF)-based VT techniques were employed for serving multiple users at the same time in the overlapping area, which will be exemplified in Section II-C.

[2] A single UE represents a communication device equipped with a VLC receiver in our down-link VLC system, which could be a smart phone, a personal computer, a tablet, a printer, etc.

all multi-user networks. However, the problem of VLC-based networks has remained to a large extent hitherto unexplored in the open literature, although recently some valuable studies were disseminated in the context of NC single-AP VLC cells [18]–[21]. In particular, the authors of [18] proposed a heuristic scheme for allocating interference-constrained sub-carriers in a multiple access VLC system relying on Discrete Multi-Tone (DMT) modulation, in order to improve the aggregate throughput. The authors of [19] carefully designed a logical framework aiming to localize, access, schedule and transmit in VLC systems, which was capable of achieving a substantial throughput at a modest complexity. However, similar to most of the literature studying resource allocation in VLC-based systems, both [18] and [19] endeavour to improve the attainable throughput without giving any cognizance to the fairness experienced by the UEs. By taking fairness into account, the authors of [20] proposed an Incremental Scheduling Scheme (ISS), where the global scheduling phase is responsible for assigning the resources to the UEs, while the local scheduling phase regularly adjusts the resource allocation by backtracking the UEs' movements. Furthermore, the authors of [21] proposed a Proportional Fairness (PF) based scheduling algorithm for a centrally controlled VLC system, which outperformed the maximum-rate scheduling policy in terms of balancing the achievable throughput against the fairness experienced by the UEs. Broadly speaking, most studies of the MUS problem encountered in VLC systems are based on single-AP VLC cells. By contrast, we are going to tackle the problems of MUS and UC-based cluster formation relying on VT.

Against the above-mentioned background, in this paper,

i) we investigate the MUS problem relying on the UEs' PF as a measure by assigning each UE a specific scheduling priority, which is inversely proportional to its anticipated resource consumption [22] and then maximizing a carefully selected network utility function [23], when jointly considering amorphous UC-VT cluster formations for the VLC down-link.

ii) More explicitly, the optimal solution of this joint UC-based cluster formation and MUS problem is first found by a high-complexity exhaustive search, which may have an overwhelming complexity even for a modest-scale system. In order to reduce the computational complexity, the original problem is formulated as a Maximum Weighted Matching (MWM) problem and multiple UEs are scheduled by solving the Kuhn-Munkres (KM) algorithm [24]–[28].

iii) To further improve the grade of practicability, a greedy algorithm is proposed, which operates at a considerably lower complexity, despite taking into account the dynamics of the UC-VT clusters.

iv) Moreover, the computational complexity of both the exhaustive search and of the proposed schemes is analysed and various cluster formations are evaluated for diverse VLC characteristics, such as the Field-Of-View (FOV), the Line-Of-Sight (LOS) blocking probabilities, the optical AP arrangement, etc.

VLC can be considered as a new member in the small-cell family of the Heterogeneous Network (HetNets) landscape for complementing the overloaded radio frequency band [17]. The UC cluster formation principle designed for VLC environments constitutes a novel and competitive design paradigm for the super dense multi-tier cell combinations of HetNets, where the sophisticated UEs can actively participate in cell planning, resource management, mobility control, service provision, signal processing, etc. Considering the large-scale multi-input-multi-output systems for example, the antenna selection scheme or beamforming techniques may be designed in a similar UC manner, according to the UEs' geo-location and service requirements. As a result, the UC concept may be expected to become one of the disruptive techniques to be used in the forthcoming 5G era [17].

The rest of this paper is organized as follows. Our system model and the UC-VT clusters considered are presented in Section II. Our MUS methodology is described and evaluated in Section III and Section IV, respectively, while dynamically constructing UC-VT clusters. Finally, Section V offers our conclusions.

II. System Model

The VLC down-link is considered, which is constituted by a set of VLC APs and each of them relies on an LED array constructed from several LEDs. The essence of our UC-VT cluster formation is to assign the UEs and optical APs to each other for the sake of maximizing the total utility after employing VT in each of the UC-VT cluster. This procedure is entirely based on the UEs' specific conditions and thus leads to UC clusters. In this section, we first discuss the optical link characteristics and cluster formation, before investigating how to select the UE set supported by a specific AP set in a multi-user system.

A. Link Characteristics

Since each UE has a limited FOV, they can only receive information from the optical APs, when one or more APs reside within the UE's FOV. According to [29], if the angle of incidence ψ from an AP to a UE is less than the UE's FOV ψ_{F}, the optical channel's Direct Current (DC) attenuation of the LOS path is given by

$$h_d = \frac{(m+1)D_{\mathrm{PA}}}{2\pi l^2}\cos^m(\phi)T_s(\psi)g(\psi)\cos(\psi), \qquad (1)$$

where the Lambert index m depends on the semi-angle $\phi_{1/2}$ at half-illuminance of the source, which is given by $m = -1/\log_2(\cos\phi_{1/2})$. Furthermore, D_{PA} is the physical area of the detector's Photo-Diode (PD), l is the distance between the VLC transmitter and the receiver, while ϕ is the angle of irradiance. Still referring to (1), $T_s(\psi)$ and $g(\psi)$ denote the gain of the optical filter and of the optical concentrator employed, respectively, while $g(\psi)$ can be written as $g(\psi) = n^2/\sin^2\psi_{\mathrm{F}}$ [29], where n is the refractive index of a lens at a PD. Furthermore, according to [10], when the incidence angle ψ is no larger than the FOV, the channel's DC attenuation on the first reflection is given by

$$dh_r = \frac{(m+1)D_{\mathrm{PA}}}{2\pi^2 l_1^2 l_2^2}\rho dD_{\mathrm{wall}}\cos^m(\phi)\cos(\beta_1)\cos(\beta_2)T_s(\psi)g(\psi)\cos(\psi), \qquad (2)$$

TABLE I: VLC Parameters

Semi-angle at half power ($\phi_{1/2}$)	70°
Modulation bandwidth (B) [7]	20 [MHz]
Physical area of a PD (D_{PA})	1.0 [cm^2]
Gain of an optical filter ($T_s(\psi)$)	1.0
Refractive index of a lens at a PD (n)	1.5
O/E conversion efficiency (γ)	0.53 [A/W]

where l_1 denotes the distance between an AP and a reflective point, while l_2 is the distance between this point and a UE. The reflectance factor and the reflective area are denoted by ρ and dD_{wall}, respectively. Additionally, β_1 and β_2 represent the irradiance angles to the reflective point and to the UE, respectively. Our VLC parameter values are summarized in TABLE I.

B. Cluster Formation

Following the traditional cellular design principle, each optical AP illuminates an individual cell and adopts Unity Frequency Reuse (UFR) across all cells, where the ICI is imposed by the LOS ray of neighbouring cells and consequently the UE may experience dramatic performance degradation at the cell edge. In order to reduce the ICI, appropriate FR patterns may be employed as an appealingly simple solution, while the system has to obey the classic trade-off between reduced bandwidth efficiency and improved cell-edge Signal-to-Interference-plus-Noise-Ratio (SINR), when using a FR factor higher than one, as investigated in our previous work [12]. Apart from the single-AP cells, we studied multi-AP merged cells, where several neighbouring VLC APs cooperate by employing either CT or VT techniques. The above-mentioned cell designs, including regular UFR/FR and merged multi-AP cells with CT/VT, rely on a fixed cell-shape, regardless of the traffic requirements, which are referred to as NC formations. In contrast to the fixed-shape NC cell formation designs, the UC design philosophy was proposed in [15]–[17], which was capable of supporting irregular-shape elastic cell formations that were capable of accommodating dynamic traffic requirements. By employing CT, each multi-AP UC-CT cell of [15] is only capable of supporting a single UE in a specific time slot. In order to serve multiple UEs at the same time, we propose the VT aided UC cluster formation, which is referred to as a UC-VT cluster in this paper. Let us now discuss the model of our system in more detail.

Fig. 1a shows the example of a particular VLC downlink network having $N_A = 16$ optical APs and $N_U = 10$ UEs, where all LOS links are denoted by dotted lines and for simplicity, the reflections are not shown. Let us first construct the link's bipartite graph $\mathcal{G}(\mathcal{V}, \mathcal{E})$, as shown in Fig. 2a, for the network of Fig. 1a. The vertex set $\mathcal{V}$ denoting the communication nodes is divided into two subsets, i.e. the optical AP set $\mathcal{V}_A$ as well as the VLC UE set $\mathcal{V}_U$, where we

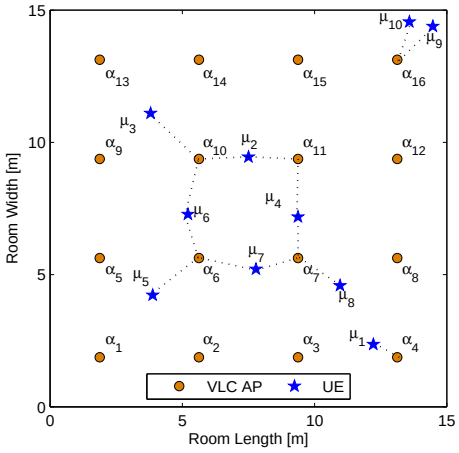

(a)

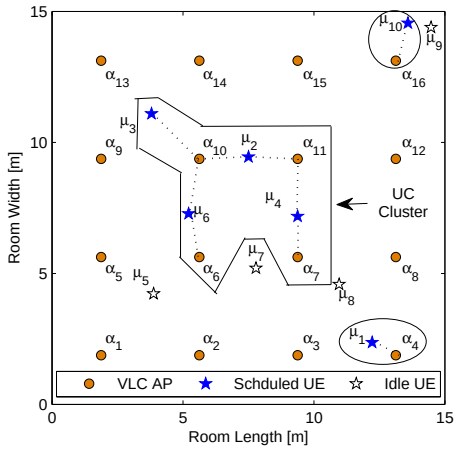

(b)

Fig. 1: (a) Layout of the VLC APs and UEs projected on the horizontal plane, where α_i and μ_j represent the VLC APs and UEs, respectively. All LOS links are denoted by dotted lines and for simplicity, the reflections are not shown in this figure. There are $(4 \times 4) = 16$ APs and 10 UEs. (b) The cluster formation result provided by Fig. 5d for the VLC system of (a).

have

$$\begin{aligned}\mathcal{V} &= \mathcal{V}_A \cup \mathcal{V}_U \\ &= \{\alpha_i | i = 1, 2, \cdots, N_A\} \cup \{\mu_j | j = 1, 2, \cdots, N_U\}, \end{aligned} \quad (3)$$

with α_i and μ_j denoting the index of VLC APs and UEs, respectively. Hence, the number of vertices in $\mathcal{G}$ is given by $(N_A + N_U)$. Furthermore, when a UE can receive data from an AP, either via the direct LOS path or via the reflected path, a link may be established between them, which is said to be an *edge*, and these two vertices are said to be *adjacent*. The edge set $\mathcal{E}$ represents all possible links between APs and UEs with one of the endpoints in $\mathcal{V}_A$ and the other one in $\mathcal{V}_U$, which may be written as

$$\mathcal{E} = \{e_{\alpha_i, \mu_j} | \alpha_i \in \mathcal{V}_A, \mu_j \in \mathcal{V}_U\}, \quad (4)$$

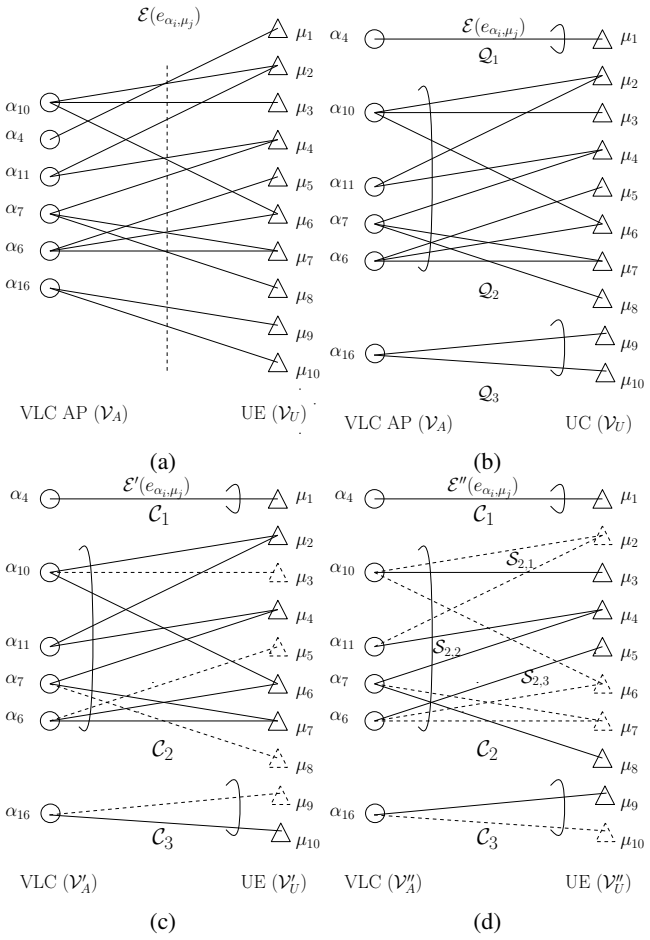

Fig. 2: (a) A graph model $\mathcal{G}(\mathcal{V},\mathcal{E})$ of the VLC down-link seen in Fig. 1a. (b) The three independent components of $\mathcal{G}$, i.e. $\mathcal{Q}_1$, $\mathcal{Q}_2$ and $\mathcal{Q}_3$. (c) and (d) Possible UC-VT cluster formations of the network. In (d), $\mathcal{S}_{2,1}$, $\mathcal{S}_{2,2}$ and $\mathcal{S}_{2,3}$ are disjoint, but they are regarded as a merged large cluster $\mathcal{C}_2$.

where e_{α_i,μ_j} denotes the link between AP α_i and UE μ_j. Since the placement of the VLC APs is fixed, the edge set is determined by the UEs' specific conditions, such as their FOV, position, etc. Therefore, the network graph is said to be UC.

Still referring to Fig. 2a, the graph $\mathcal{G}$ is not fully *connected*, since not all pairs of vertices are joined by a path. Further scrutiny reveals that $\mathcal{G}$ has three independent components, which are said to be partially *connected components*, as explicitly shown in Fig. 2b, marked by $\mathcal{Q}_1$, $\mathcal{Q}_2$ and $\mathcal{Q}_3$. There are no adjacent AP-UE vertices amongst these distinctive components of $\mathcal{Q}_1$, $\mathcal{Q}_2$ and $\mathcal{Q}_3$, which indicates that UEs cannot receive data from the optical APs belonging to the other components, only from their own. Thus, the ICI is totally eliminated. Explicitly, since none of the individual components is affected by the others, the proposed cluster formation algorithms may be executed within every single component, as it will be discussed in Section III. On the other hand, in order to simultaneously serve multiple UEs, Zero-Forcing (ZF)-based VT techniques are introduced in our system. The underlying principle of ZF-based VT is to totally eliminate the interference at the multiple AP transmitters, so that all the UEs receive mutually interference-free signals. In general, when employing VT the maximum number of UEs supported in a single time slot should be no more than the number of APs. Hence, the ZF-based VT may not be employed directly by each component in Fig. 2b. For example, the number of UEs is almost twice as high as the number of APs in $\mathcal{Q}_2$. Therefore, we eliminate the interference by ensuring that only some of the UEs will be scheduled and we solve this problem by constructing a UC-VT cluster with the aid of the serving APs. There are various options for scheduling the UEs shown in Fig. 2c and 2d, where the UEs denoted by the dashed triangle boundary are not scheduled and the edges denoted by dashed lines are not established during the current slot. Furthermore, the UC-VT clusters formed are denoted by $\mathcal{C}_n$, i.e. by $\mathcal{C}_1$, $\mathcal{C}_2$ and $\mathcal{C}_3$ in Fig. 2c and 2d. Before investigating how to schedule the UEs, let us first discuss the VT within each UC-VT cluster formed.

C. Vectored Transmission

After scheduling the UEs, each UC-VT cluster is formed, as shown for example in Fig. 2c, where the clusters are denoted by $\mathcal{C}_1$, $\mathcal{C}_2$ and $\mathcal{C}_3$, respectively. Within $\mathcal{C}_1$ or $\mathcal{C}_3$, only a single UE is supported by a single AP, which is a similar scenario to the regular NC design. However, in order to allow $\{\alpha_{10},\alpha_{11},\alpha_7,\alpha_6\}$ to simultaneously serve all the UEs $\{\mu_2,\mu_4,\mu_6,\mu_7\}$ within $\mathcal{C}_2$, we employ Zero-Forcing (ZF)-based VT techniques. More explicitly, we may write the channel's attenuation $\boldsymbol{H}_{\mathcal{C}_2}$ between the multiple APs and UEs within $\mathcal{C}_2$ as:

$$\boldsymbol{H}_{\mathcal{C}_2} = \begin{array}{c} \\ \mu_2 \\ \mu_4 \\ \mu_6 \\ \mu_7 \end{array} \begin{array}{c} \begin{array}{cccc} \alpha_{10} & \alpha_{11} & \alpha_7 & \alpha_6 \end{array} \\ \begin{pmatrix} h_{11} & h_{12} & 0 & 0 \\ 0 & h_{22} & h_{23} & 0 \\ h_{31} & 0 & 0 & h_{34} \\ 0 & 0 & h_{43} & h_{44} \end{pmatrix} \end{array}. \tag{5}$$

In order to attain mutually interference-free signals at the receivers, the transmitted signals $\boldsymbol{X}_{\mathcal{C}_2} = [x_1, x_2, x_3, x_4]$ are precoded as $(\boldsymbol{P}_{\mathcal{C}_2} \cdot \boldsymbol{X}_{\mathcal{C}_2})$ and we may write $\boldsymbol{P}_{\mathcal{C}_2} = (\boldsymbol{G}_{\mathcal{C}_2} \cdot \boldsymbol{\Omega}_{\mathcal{C}_2})$, where the matrix $\boldsymbol{G}_{\mathcal{C}_2} = \boldsymbol{H}^H_{\mathcal{C}_2} \cdot (\boldsymbol{H}_{\mathcal{C}_2} \cdot \boldsymbol{H}^H_{\mathcal{C}_2})^{-1}$ obeys the ZF criterion for the sake of obtaining an interference-free identity matrix for $\boldsymbol{H}_{\mathcal{C}_2} \cdot \boldsymbol{G}_{\mathcal{C}_2} = \boldsymbol{I}_4$ and $\boldsymbol{\Omega}_{\mathcal{C}_2}$ is introduced in order to satisfy the power constraint. Hence, the ICI can be totally eliminated at the multiple AP transmitters and as a result, all the UEs receive mutually interference-free signals. Let us now elaborate on the VT techniques a little further in general terms and derive the formations of $\boldsymbol{G}$ and $\boldsymbol{\Omega}$.

Each UC-VT cluster $\mathcal{C}_n$ is constituted by a set of APs $\mathcal{V}_{A,\mathcal{C}_n}$ with a cardinality of $N_{A,\mathcal{C}_n}$ and a set of UEs $\mathcal{V}_{U,\mathcal{C}_n}$ with a cardinality of $N_{U,\mathcal{C}_n}$. Let further $\boldsymbol{X}_t \in \mathbb{R}^{N_{U,\mathcal{C}_n}\times 1}$ and $\boldsymbol{Y}_r \in \mathbb{R}^{N_{U,\mathcal{C}_n}\times 1}$ denote the vectors of transmitted and received signals, respectively. Upon using VT, we have

$$\boldsymbol{Y}_r = \gamma \cdot P_t \cdot \boldsymbol{H} \cdot \boldsymbol{G} \cdot \boldsymbol{\Omega} \cdot \boldsymbol{X}_t + \boldsymbol{N}, \tag{6}$$

where γ and P_t denote the Optical/Electronic (O/E) conversion efficiency and the transmitted optical power, respectively. Furthermore, $\boldsymbol{N}$ denotes the noise, while the channel-matrix $\boldsymbol{H} \in \mathbb{R}^{N_{U,\mathcal{C}_n}\times N_{A,\mathcal{C}_n}}$ hosts the DC attenuations between the

$N_{U,\mathcal{C}_n}$ UEs and the $N_{A,\mathcal{C}_n}$ APs, while the matrix $\boldsymbol{G} = \boldsymbol{H}^H \cdot (\boldsymbol{H} \cdot \boldsymbol{H}^H)^{-1}$ obeys the ZF criterion, which hence results in a beneficial interference-free identity matrix for $\boldsymbol{H} \cdot \boldsymbol{G} = \boldsymbol{I}_{N_{U,\mathcal{C}_n}}$. Finally, the matrix $\boldsymbol{\Omega}$ is introduced to enforce the per-AP power constraints, hence we have

$$\boldsymbol{\Omega} = \varphi \boldsymbol{I}_{N_{U,\mathcal{C}_n}}, \quad \varphi = \min_{i=1,2,\ldots,N_{A,\mathcal{C}_n}} \sqrt{\frac{1}{\|\boldsymbol{G}(i,:)\|_F^2}}, \tag{7}$$

where $\boldsymbol{G}(i,:)$ is the ith row of $\boldsymbol{G}$. To elaborate a little further, assuming that we have the per-AP optical power constraint of P_t, the signal transmitted with the equal power from the ith AP is $\varphi^2 \|\boldsymbol{G}(i,:)\|_F^2$. Note that we have $P_e = \pi P_t^2$, when considering the Asymmetrically-Clipped Optical OFDM (ACO-OFDM) [8]. Hence, we have $\varphi^2 \|\boldsymbol{G}(i,:)\|_F^2 \leq \pi P_t^2 \Rightarrow \varphi \leq \pi P_t^2 / \sqrt{\|\boldsymbol{G}(i,:)\|_F^2}$. In order to let each AP satisfy the power constraint, we have $\varphi = \min_i \pi P_t^2 / \sqrt{\|\boldsymbol{G}(i,:)\|_F^2}$, as indicated in (7). Furthermore, let us define the SINR as the aggregate electronic power over the noise power in a bandwidth of B [MHz] [7] plus the sum of the electronic power received from other optical sources in the vicinity. Since the corresponding electronic power is proportional to the square of the electronic current's amplitude and both the intra-cluster and inter-cluster LOS interferences are mitigated, we may express the SINR for a particular UE μ_j within the cluster $\mathcal{C}_n$ as

$$\xi = \frac{\gamma^2 P_t^2 \varphi^2 \pi}{N_0 B + I_r}, \tag{8}$$

where I_r is the interference imposed by the reflected light. Since the interference power received by the cluster under consideration is influenced by the ZF-based VT within other clusters, for simplicity, we assume that the interference imposed is always equal to its maximum value, which characterizes the worst-case situation in our VT cluster formations. Furthermore, N_0 [A^2/Hz] is the noise power spectral density dominated by the shot noise N_{shot} [10] given by $N_0 \cong N_{\text{shot}} = qI_a(P_r) \sim 10^{-22}$, where q denotes the electron charge and $I_a(P_r)$ is the photo-current at the receiver [7].

Note that there are two popular techniques of constructing white LEDs, namely either by mixing the Red-Green-Blue (RGB) frequencies using three chips, or by using a single blue LED chip with a phosphor layer. We consider the latter one, which is the favoured commercial version. Although the terminology of 'white' LED gives the impression of having all frequency components across the entire visible light spectrum, in fact only the blue frequency-range is detected. More explicitly, not even the entire blue frequency-range is detected, since the less responsive phosphorescent portion of the frequency-band is ignored. Hence, the modulation bandwidth is typically around 20 MHz, albeit this measured bandwidth depends on the specific LED product used. Given this 20 MHz bandwidth, we are now ready to employ ACO/DC biased Optical (DCO)-OFDM and partition it into arbitrary frequency reuse patterns.

III. Methodology

Let us now schedule multiple UEs in the VLC system in a PF manner by taking into account our UC-VT cluster formation, which is ultimately a joint UC-VT cluster formation and MUS problem. In this section, we commence with a general formulation of this joint problem and then propose an exhaustive search method, which finds the optimal solution maximizing the aggregate utility of the VLC system considered. In order to reduce the computational complexity imposed, the original problem is reformulated as an MWM problem, whose optimal solution is provided by the classic KM-algorithm-based [24] approach. For further simplifying the MUS process, we propose a greedy scheduling algorithm for finding a suboptimal solution for our original joint problem, whilst imposing a significantly reduced complexity. Note that for simplicity, we only consider LOS links in terms of constructing UC-VT clusters. By contrast, in addition to the LOS component, the effect of the first reflection will also be considered, when calculating both the UEs' SINR and the achievable data rate, as indicated in (8). However, our algorithm is a generic one, which may be readily applied, when considering the reflected light for UC-VT cluster formation.

A. Problem Formulation

Our goal is to find the optimal UC-VT cluster formation for maximizing the long-term network-wide utility, while scheduling UEs in a PF manner, which is ultimately a joint cluster formation and MUS problem. In order to implement a PF scheduler, the weight of each link between APs and UEs may be defined as

$$\omega(e_{\alpha_i,\mu_j}) = \frac{r_{\alpha_i,\mu_j}}{\hat{r}_{\mu_j}}, \quad e_{\alpha_i,\mu_j} \in \mathcal{E}, \tag{9}$$

where r_{α_i,μ_j} denotes the achievable data rate of the UE μ_j from the AP α_i during the current slot. Since the SINR ξ experienced by a particular UE is determined by the channel attenuation matrix (5) between the APs and UEs within the cluster, r_{α_i,μ_j} should be a function of the cluster formation, which may be written as:

$$r_{\alpha_i,\mu_j} = f(\mathcal{E}'), \quad e_{\alpha_i,\mu_j} \in \mathcal{E}', \mathcal{E}' \subseteq \mathcal{E}, \tag{10}$$

where $\mathcal{E}'$ is the set of established links, after the UEs have been scheduled and the UC-VT clusters have been constructed. Furthermore, $\hat{r}_{\mu_j}$ denotes the long-term average throughput of the UE μ_j, which may be obtained over a time window T_F as a moving average according to [30]:

$$\hat{r}_{\mu_j}^{(t)} = \begin{cases} (1 - \frac{1}{T_{\text{F}}}) \hat{r}_{\mu_j}^{(t-1)} + \frac{1}{T_{\text{F}}} r_{\alpha_i,\mu_j}^{(t)}, & \text{if scheduled,} \\ (1 - \frac{1}{T_{\text{F}}}) \hat{r}_{\mu_j}^{(t-1)}, & \text{if not scheduled.} \end{cases} \tag{11}$$

For a given UC-VT cluster formation $\{\mathcal{C}_n\}$, the aggregate utility may be formulated by taking into account the weight of each edge, where again, the weight physically represents the PF scheduling priority of the link [30], which is formulated as:

$$\begin{aligned} W &= \sum_{e_{\alpha_i,\mu_j} \in \mathcal{E}'} \omega(e_{\alpha_i,\mu_j}) \\ &= \sum_{\alpha_i \in \mathcal{V}_A'} \sum_{\mu_j \in \mathcal{V}_U'} \frac{r_{\alpha_i,\mu_j}}{\hat{r}_{\mu_j}}, \quad \mathcal{E}' \subseteq \mathcal{E}, \end{aligned} \tag{12}$$

where $\mathcal{V}'_A$ and $\mathcal{V}'_U$ denote the serving APs and the scheduled UEs set, respectively. It is plausible that various UC-VT cluster formations may lead to different total utility. The maximum value of the aggregate utility W may be achieved by finding the optimal cluster formation. Thus, our problem may be described as selecting an appropriate set of edges $\mathcal{E}^*$ from $\mathcal{E}$ and then forming several UC-VT clusters, which maximizes (12). Hence, our Objective Function (OF) may be formulated as:

$$\mathcal{E}^* = \arg\max_{\mathcal{E}' \subseteq \mathcal{E}}(W) = \arg\max_{\mathcal{E}' \subseteq \mathcal{E}} \left(\sum_{\alpha_i \in \mathcal{V}'_A} \sum_{\mu_j \in \mathcal{V}'_U} \frac{r_{\alpha_i,\mu_j}}{\hat{r}_{\mu_j}} \right). \tag{13}$$

Note that in (13) we focus our attention on the aggregate utility of the entire system and do not distinguish, which particular APs and UEs belong to which UC-VT clusters. Let us now discuss the constraint of (13), from the perspective of a single UC-VT cluster. As mentioned in Section II-B, the number of scheduled UEs should not exceed the service capability of a cluster employing VT, where again, the maximum number of UEs supported is equal to the number of APs. Hence, within a single UC-VT cluster $\mathcal{C}_n$ we have

$$N_{A,\mathcal{C}_n} \geq N_{U,\mathcal{C}_n}. \tag{14}$$

For solving (13) under the constraint of (14) and finding the optimal cluster formation, we have to know the weight of all edges in $\mathcal{E}$. However, according to (9), the weight $\omega(e_{\alpha_i,\mu_j})$ of a particular link is defined as a function of the data rate achieved by one of its endpoints μ_j during its reception from the other endpoint α_i, which can only be determined after all clusters have been formed, as briefly introduced in Section II-C. To the best of our knowledge, the optimal solution of this joint problem may only be found via exhaustive search.

B. Optimization of the Joint Problem

Given a VLC network topology having N_A optical APs and N_U UEs, it may be composed of some independent components, for example as shown in Fig. 2b. Note that these naturally disjoint components of the network may not constitute the final formations of the UC-VT cluster. More explicitly, there is no limitation concerning the number of APs and UEs within each single component of the network, apart from the fact that within a UC-VT cluster the cardinality of the actively served UE vertex set should be no larger than that of the AP set, as indicated by (14). Each UC-VT cluster should be an independent component of the network, where no ICI is imposed on the neighbouring clusters. Furthermore, each individual network component should be connected at the outset, but each may become disconnected and partitioned into several sub-components/clusters throughout the process of scheduling the UEs, as shown in Fig. 2d, where $\mathcal{S}_{2,1}$, $\mathcal{S}_{2,2}$ and $\mathcal{S}_{2,3}$ will be regarded as a large merged cluster.

Still referring to Fig. 2b, in order to find the optimal cluster formation for maximizing (12), the optimization is performed separately in $\mathcal{Q}_1$, $\mathcal{Q}_2$ and $\mathcal{Q}_3$, which are independent network components. Within $\mathcal{Q}_1$, only a single UE μ_1 is capable of connecting with the AP α_4, where α_4 either supports μ_1 or it will be turned off. Therefore, there are two AP-UE combination scenarios for $\mathcal{Q}_1$. Within $\mathcal{Q}_2$, there are three UEs, i.e. μ_2, μ_3 and μ_6, which are within the coverage of the AP α_{10}. Hence, α_{10} may either select one of them to support or become inactive. Thus, there are $(3+1)$ choices for α_{10}. Similarly, the other APs α_{11}, α_7 and α_6 have $(2+1)$, $(3+1)$ and $(3+1)$ choices, respectively. Therefore, the number of possible AP-UE combinations within $\mathcal{Q}_2$ is $(4 \times 3 \times 4 \times 4 = 192)$. $\mathcal{Q}_3$ has an easier situation, where the AP α_{16} may either select one UE from $\{\mu_9, \mu_{10}\}$ or opts for providing no services. For the entire network of Fig. 2b, the number of possible AP-UE combinations becomes $((2-1)+(192-1)+(3-1) = 194)$. Finally, we take into account the undesired scenario, where all APs are out of service by subtracting 1. Generally speaking, our exhaustive search-based approach of finding the optimal UC-VT cluster formation is detailed below.

i) For each separate network component $\mathcal{Q}_m$ relying on $N_{A,\mathcal{Q}_m}$ APs and $N_{U,\mathcal{Q}_m}$ UEs, let $N^{\alpha_i}_{U,\mathcal{Q}_m}$ denote the number of possible links between a certain AP α_i with the UEs within its coverage, where $i = 1, 2, \cdots, N_{A,\mathcal{Q}_m}$.

ii) Note that not the entire set of APs has to be active during the scheduling process. In other words, we do not limit the number of active APs or scheduled UEs, when aiming for finding the optimal cluster formation. Thus the concept of a *virtual* link is introduced for each AP, which theoretically exists, but it is turned off. Hence, the number of possible AP-UE combinations in $\mathcal{Q}_m$ may be expressed as

$$\prod_{i=1}^{N_{A,\mathcal{Q}_m}} (N^{\alpha_i}_{U,\mathcal{Q}_m} + 1) - 1, \tag{15}$$

where we have $1 \leq N^{\alpha_i}_{U,\mathcal{Q}_m} \leq N_{U,\mathcal{Q}_m}$. Note that in (15), subtracting 1 implies that we have removed the undesired scenario, where all APs are turned off.

iii) For each possible UC-VT cluster formation in $\mathcal{Q}_m$, the aggregate utility can be calculated and the optimal formation associated with the maximum utility is found correspondingly. Since each network component $\mathcal{Q}_m$ is independent, the optimal cluster formation is separately found in each of them. Hence, for finding the optimal solution of (13) for the entire system, we need to repeat the process of ii) in each $\mathcal{Q}_m$. Thus the total number of possible AP-UE combinations is the summation of (15) for each $\mathcal{Q}_m$, which may be expressed as

$$\sum_m \left(\prod_{i=1}^{N_{A,\mathcal{Q}_m}} (N^{\alpha_i}_{U,\mathcal{Q}_m} + 1) - 1 \right). \tag{16}$$

The number of all possible cluster formations within a single scheduling time slot at a ms-based scale is given by (16), which is jointly determined by the number of APs ($N_{A,\mathcal{Q}_m}$) and number of UEs ($N_{U,\mathcal{Q}_m}$) as well as by the specific distribution of the UEs ($N^{\alpha_i}_{U,\mathcal{Q}_m}$). For a network associated with a low density of UEs and a small number of APs, a desirable cluster formation solution may be achieved by exhaustively searching all the possibilities. For example, when 16 APs support 10 UEs, the optimal association will be found after searching $\sim 10^4$ possible cluster formations. However, this

search-space may become excessive within a time slot at a ms-based scale even for a modest-scale network, which makes the exhaustive search strategy unacceptable owing to its computational complexity. For example, as many as $\sim 10^7$ cluster formations have to be searched within a single processing time slot, when there are 20 UEs supported by 16 APs. Hence, instead of solving the joint problem directly, we update the definition of the weight for each link and reformulate the original problem with the goal of significantly reducing the complexity, as it will be detailed in Section IV.

C. Distance-based Weight and Problem Reformulation

In (9), the weight of each link is related to the UE's achievable data rate, which cannot be determined before the UC-VT clusters have finally been constructed. Our ultimate goal is that of finding the optimal cluster formation based on the sum weight attained by appropriately scheduling the UEs, as indicated by (13). In other words, the cluster formation and MUS problems were originally coupled. Hence, we opt for simplifying the original problem by adopting a deterministic weight for each AP-UE link. Thus, the maximization of the sum weight may be realized before the UC-VT clusters are constructed, and as a benefit, the joint cluster formation and MUS problem becomes decoupled.

As mentioned in Section III-B, the weight of each link between the AP and the UE is non-deterministic, which is influenced by how the UC-VT clusters are constructed, while the optimal cluster formation solution is determined by maximizing the sum weight of all the scheduled links. Hence, we opt for bypassing the non-deterministic weight assignment and instead, we opt for selecting active links according to their optical channel quality, which is significantly affected by the UE's position, according to (1). We directly adopt each UE's position information for determining the weight of each link and introduce a new weighted bipartite graph $\mathcal{G}_d(\mathcal{V}, \mathcal{E})$, which is constructed based on the original graph $\mathcal{G}(\mathcal{V}, \mathcal{E})$ and they have the same vertex and edge sets. However, the weight of each edge is redefined as

$$\omega_d(e_{\alpha_i,\mu_j}) = \frac{1/l^3_{\alpha_i,\mu_j}}{\hat{r}_{\mu_j}}, \quad e_{\alpha_i,\mu_j} \in \mathcal{E}, \tag{17}$$

where l_{α_i,μ_j} represents the distance between the AP α_i and the UE μ_j. Given that the APs are fixed, the weight is determined by the specific position of each UE μ_j. It can be readily seen from (1) that the VLC links having a shorter length have a better channel quality. Therefore, the weight is inversely proportional to the distance and thus the links associated with better channels have a higher weight. Note that if the UE μ_j is too far away from the AP α_i, namely μ_j is not within the coverage of α_i, it is reasonable to assume having $\omega_d(e_{\alpha_i,\mu_j}) = 0$.

Our problem becomes that of selecting a subset of links $\mathcal{E}^*_d$ having a better channel quality, and along with their endpoints they represent our UC-VT cluster formation. In general, within a UC-VT cluster, multiple APs serve multiple UEs and there may not be a one-to-one relationship. Nonetheless, in the first MUS step, we could select the one-to-one AP-UE pairs according to their distance-based weight, where the serving APs and the scheduled UEs are determined. Then, in the cluster formation step, the cluster may be constructed by adding other possible links between the selected AP-UE set. Thus the MUS and cluster formation problem is decoupled and solved separately. Note that in the MUS step, a specific set of the links between all the AP-UE pairs, which do not share the same AP or UE, is said to represent independent edges and they constitute a *matching* $\mathcal{M}$ defined over the graph. For example, in Fig. 2b we have 6 AP vertices plus 10 UE vertices as well as 14 edges. In order to construct a matching, 6 UEs are selected and each of them matches a specific AP associated with one edge, e.g. $\{\alpha_4 \to \mu_1, \alpha_{10} \to \mu_3, \alpha_{11} \to \mu_4, \alpha_7 \to \mu_7, \alpha_6 \to \mu_6, \alpha_{16} \to \mu_9\}$. Furthermore, we have $\mathcal{M} \subseteq \mathcal{E}^*_d \subseteq \mathcal{E}$. To elaborate a litter further in general terms, let us first formally define the matching over a graph. As mentioned in Section III-B, the network graph model may be disconnected and divided into multiple independent components. For an individual component, denoted by $\mathcal{Q}_m(\mathcal{V}_{\mathcal{Q}_m}, \mathcal{E}_{\mathcal{Q}_m})$, which is a subgraph of $\mathcal{G}_d$ associated with the vertex set $\mathcal{V}_{\mathcal{Q}_m}$ and the edge set $\mathcal{E}_{\mathcal{Q}_m}$, a matching $\mathcal{M}_{\mathcal{Q}_m}$ may be defined as a specific subset of the edge set $\mathcal{E}_{\mathcal{Q}_m}$, where no pair of edges shares a vertex within $\mathcal{M}_{\mathcal{Q}_m}$. It is plausible that the cardinality of the edge-subset $\mathcal{M}_{\mathcal{Q}_m}$ is given by the number of the $\mathcal{M}_{\mathcal{Q}_m}$-saturated AP/UE vertices, which belongs to the edges of $\mathcal{M}_{\mathcal{Q}_m}$. Otherwise, the vertices not belonging to the edges of $\mathcal{M}_{\mathcal{Q}_m}$ are said to be $\mathcal{M}_{\mathcal{Q}_m}$-unsaturated. Hence, if we allow as many UEs as possible to be scheduled, $\mathcal{M}$ should have the highest possible cardinality. Furthermore, considering the weight of each edge, our cluster formation problem may be further reformulated as a MWM problem, where the OF may be written as:

$$\begin{aligned} \mathcal{M}^*_{\mathcal{Q}_m} &= \arg\max_{\mathcal{M}_{\mathcal{Q}_m}} (W_{\mathcal{Q}_m}) \\ &= \arg\max_{\mathcal{M}_{\mathcal{Q}_m}} \left(\sum_{\alpha_i \in \mathcal{V}_{\mathcal{Q}_m}, \mu_j \in \mathcal{V}_{\mathcal{Q}_m}} \omega_d(e_{\alpha_i,\mu_j}) \right). \end{aligned} \tag{18}$$

Upon solving (18) within each individual network component, a set of APs as well as UEs is selected in order to form a UC-VT cluster along with all links between them. Thus, the solution of the MWM problem is expected to provide a suboptimal result for our original joint MUS and UC-VT cluster formation problem, which is however found at a significantly reduced complexity.

D. Optimal MWM

If we construct a $(N_{A,\mathcal{Q}_m} \times N_{U,\mathcal{Q}_m})$-element weight matrix $(\omega_d(e_{\alpha_i,\mu_j}))$ for each of the individual component $\mathcal{Q}_m$, the problem of (18) may be viewed as being equivalent to finding a set of independent elements from $(\omega_d(e_{\alpha_i,\mu_j}))$, in order to maximize the sum of these elements. The definition of independent elements indicates that none of them occupies the same row or column, where a row represents an AP and a column represents a UE. To be more explicit, the selected set of the independent elements in the weight matrix corresponds to a matching of the graph, since a single element represents an edge of the graph and no pair of these elements shares

the same AP or UE. Thus our MWM problem has also been interpreted in a matrix form. Before finding the optimal solution of the afore-mentioned MWM problem, let us first introduce Theorem 1.

Theorem 1. *Given the* $(n_r \times n_r)$*-element matrix* (a_{ij}) *and* (b_{ij})*, as well as the column vector* (c_i) *and the row vector* (r_j)*, satisfying* $b_{ij} = c_i + r_j - a_{ij}$*, provided the permutation* p $(p_i : i = 1, \cdots, n_r)$ *of the integers* $1, \cdots, n_r$ *minimizes* $\sum_{i=1}^{n_r} a_{ip_i}$*,* p *then also maximizes* $\sum_{i=1}^{n_r} b_{ip_i}$*.*

Proof: Let p be a permutation of the integers 1,2, $\cdots$, n minimizing $\sum_{i=1}^{n_r} a_{ip_i}$, then we have

$$\sum_{i=1}^{n_r} b_{ip_i} = \sum_{i=1}^{n_r} c_i + \sum_{i=1}^{n_r} r_{p_i} - \sum_{i=1}^{n_r} a_{ip_i}.$$

Since the first two terms are constant and independent of p, $\sum_{i=1}^{n_r} b_{ip_i}$ is maximized, when $\sum_{i=1}^{n_r} a_{ip_i}$ is minimized by p. ■

Hence, if we want to find the optimal assignment solution for maximizing $\sum_{i=1}^{n} b_{i,p_i}$, what we have to do is to transform (b_{ij}) into (a_{ij}) as mentioned above and then find the optimal solution minimizing $\sum_{i=1}^{n} a_{i,p_i}$, where (a_{ij}) and (b_{ij}) are said to be *equivalent*. For a rectangular $(n_r \times n_c)$-element matrix (a'_{ij}), we can obtain a square matrix (a_{ij}) by attaching $|n_r - n_c|$ lines of zero elements to (a'_{ij}). Thus, (a'_{ij}) and (a_{ij}) have the same optimal assignment solution and Theorem 1 can be readily applied for non-square rectangular matrices, where we have $n_r \neq n_c$.

In order to solve our MWM problem, which is derived from our joint cluster formation and MUS problem, we introduce the classic Kuhn-Munkres (KM) algorithm [24], [25], which is an efficient method of solving the matching problems of bipartite graphs and may be readily applied in a symmetric graph. However, the number of VLC UEs is usually higher than that of the optical APs within a single network component $\mathcal{Q}_m$, which results in an asymmetric bipartite graph. Owing to the efforts of Bourgeois and Lassalle [26], an extension of the KM algorithm was developed for non-square rectangular matrices. Relying on this approach, we introduce a KM-algorithm-based technique of solving our UC-VT cluster formation problem. The mathematical formulation of the extended KM algorithm of [26] may be described as that of finding a set of k independent elements $k = \min\{n_r, n_c\}$ from a given $(n_r \times n_c)$-element matrix $(b_{i,j})$, in order to minimize the sum of these elements. However, our problem is not a minimization, but a maximization problem associated with the OF of (18). Therefore, we first transform our MWM problem into an equivalent assignment problem based upon Theorem 1 and then invoke the KM algorithm for finding the optimal solution of the equivalent problem, which is also optimal for our MWM problem. Furthermore, since the MWM result of each naturally disjoint network component is mutually independent, the matching algorithm is executed within each individual component in a parallel manner.

As shown in Fig. 3a, $\mathcal{Q}_2$ is an independent network component and also a subgraph of our weighted graph $\mathcal{G}_d$, which also shows the individual weights of the $\{\alpha_i - \mu_j\}$ links. In order to schedule the maximum number of UEs, given the four APs in $\mathcal{Q}_2$, four of them will be selected and each one is paired with a specific AP, where the possible matchings and the corresponding sum weight values are shown in Fig. 3b. For example, bearing in mind Fig. 3a, the first matching of the first row in Fig. 3b may represent $\{\alpha_{10} \rightarrow \mu_2, \alpha_{11} \rightarrow \mu_4, \alpha_7 \rightarrow \mu_7, \alpha_6 \rightarrow \mu_5\}$, which leads to a sum weight of $W_{\mathcal{Q}} = \sum_{l=1}^{4} \omega_l = 4 + 3 + 4 + 2 = 13$. The specific matching of the seventh row in Fig. 3b is $\{\alpha_{10} \rightarrow \mu_3, \alpha_{11} \rightarrow \mu_2, \alpha_7 \rightarrow \mu_4, \alpha_6 \rightarrow \mu_6\}$, which is represented by the shaded row of Fig. 3b. This achieves the largest sum weight of $W_{\mathcal{Q}} = \sum_{l=1}^{4} \omega_l = 2 + 4 + 6 + 4 = 16$. The corresponding weights in Fig. 3a are circled. Hence they represent the optimal matching in the scenario considered.

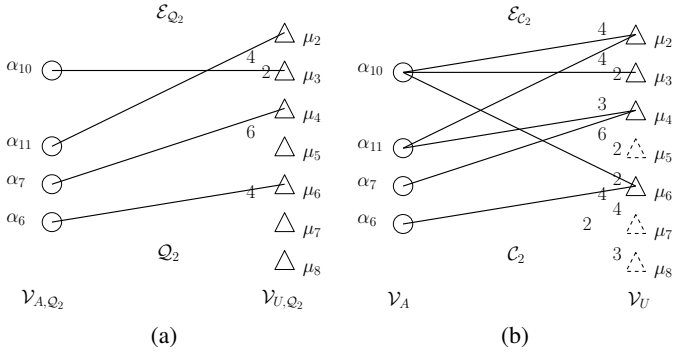

Fig. 4: (a) The optimal solution for the MWM problem (18) relying on the distance-based weight defined by (17), which is provided by the KM-algorithm-based assignment. (b) The UC-VT cluster formation based on the matching result of Fig. 3a, where more links are added for employing VT and thus the multiple APs $\{\alpha_{10}, \alpha_{11}, \alpha_7, \alpha_6\}$ are capable of supporting all the scheduled UEs $\{\mu_2, \mu_3, \mu_4, \mu_6\}$ simultaneously. The triangle with a dashed boundary denotes the specific UE, which is not scheduled during the current slot.

Instead of listing all matchings, we now proceed by constructing an equivalent minimization problem for our MWM and invoke the KM algorithm [24], [26] for finding the optimal solution, which is described in detail in Appendix A. As shown in Fig. 4a, the KM-algorithm-based approach provides the optimal solution for the MWM problem (18), with its UE-AP distance-based weight defined by (17). The matched AP-UE pairs form a UC-VT cluster and the aggregate utility in (12) can be calculated according to the matching result. However, by employing VT among the set of APs and UEs, the actual cluster may be formed with the aid of more links, as seen in Fig. 4b. Thus, the UC-VT cluster formation provided by the single-to-single matching solution may not be optimal for (13), but it is capable of offering an acceptable suboptimal solution attained at a lower complexity than that of the exhaustive search. Explicitly, it has a complexity order of $O(k^2 \times l)$ [26], where we have $k = \min\{N_{A,\mathcal{Q}_m}, N_{U,\mathcal{Q}_m}\}$ and $l = \max\{N_{A,\mathcal{Q}_m}, N_{U,\mathcal{Q}_m}\}$. The complexity of both the exhaustive search and KM algorithm will be investigated in Section IV in the context of our VLC-based network.

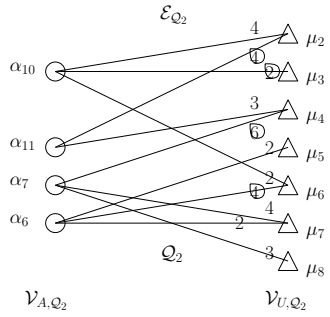

(a)

α_{10}	α_{11}	α_7	α_6	W_{Q}	α_{10}	α_{11}	α_7	α_6	W_{Q}
μ_2	μ_4	μ_7	μ_5	13	μ_3	μ_4	μ_7	μ_5	11
μ_2	μ_4	μ_7	μ_6	15	μ_3	μ_4	μ_7	μ_6	13
μ_2	μ_4	μ_8	μ_5	12	μ_3	μ_4	μ_8	μ_5	10
μ_2	μ_4	μ_8	μ_6	14	μ_3	μ_4	μ_8	μ_6	12
μ_2	μ_4	μ_8	μ_7	12	μ_3	μ_4	μ_8	μ_7	10
μ_3	μ_2	μ_4	μ_5	14	μ_6	μ_2	μ_4	μ_5	14
μ_3	μ_2	μ_4	μ_6	16	μ_6	μ_2	μ_4	μ_7	14
μ_3	μ_2	μ_4	μ_7	15	μ_6	μ_2	μ_7	μ_5	12
μ_3	μ_2	μ_7	μ_5	12	μ_6	μ_2	μ_8	μ_5	11
μ_3	μ_2	μ_7	μ_6	14	μ_6	μ_2	μ_8	μ_7	11
μ_3	μ_2	μ_8	μ_5	11	μ_6	μ_4	μ_7	μ_5	11
μ_3	μ_2	μ_8	μ_6	13	μ_6	μ_4	μ_8	μ_5	10
μ_3	μ_2	μ_8	μ_7	11	μ_6	μ_4	μ_8	μ_7	10

(b)

Fig. 3: (a) A component of $\mathcal{G}_d$, $\mathcal{Q}_2$, where the distance-based weight of each link is assumed to be as seen in (a), which is inversely proportional to the AP-UE distances in Fig. 1a with the UEs' being randomly distributed. (b) List of all possible AP-UE matchings in $\mathcal{Q}_2$ and the corresponding sum weight W_{Q}. The best matching associated with the circled weights of (a) is the one in the grey-shaded line 7.

E. Proposed Greedy Cluster Formation/MUS Algorithm

In order to further simplify the procedures of scheduling the UEs in our UC-VT cluster formation, in this section we propose a greedy cluster formation/MUS algorithm operating at a low complexity, which is also capable of achieving a near-optimal solution for our original cluster formation problem of (13). Before discussing our proposed MUS problem, let us first introduce some notations. Explicitly, $\mathcal{V}_{U,\alpha_i}$ denotes the set of UEs within the coverage of a specific AP α_i with a UE-cardinality of N_{U,α_i}. Each UE μ_j is assumed to have a scheduling priority corresponding to each AP α_i, which is given by the weight in (17). Let $\mathcal{P}_{\alpha_i} = (\omega_d(e_{\alpha_i,\mu_j} : \mu_j \in \mathcal{V}_{U,\alpha_i})$ denote the priority of each element of $\mathcal{V}_{U,\alpha_i}$ representing the AP α_i. Furthermore, if a UE does not receive any connection request from any AP during the slot considered, it is said to be an idle UE; otherwise, it is an active UE. Let us now introduce our algorithm by considering Fig. 5a, for example.

i) *Initial selection.* Each VLC AP α_i selects the specific UE $\mu_j^{\alpha_i}$ from $\mathcal{V}_{U,\alpha_i}$ associated with the highest distance-based priority, which satisfies

$$\mu_j^{\alpha_i} = \arg \max_{\mu_j \in \mathcal{V}_{U,\alpha_i}} (\mathcal{P}_{\alpha_i}). \tag{19}$$

If the UE $\mu_j^{\alpha_i}$ receives an assignment request exclusively from the AP α_i, this AP-UE pair is referred to as a Single-to-Single Matching (SSM), which may be formally defined as

$$\mathcal{M}_{\mathrm{SSM}} = \{\alpha_i \to \mu_j^{\alpha_i} : \forall \alpha_{i'} \neq \alpha_i \Rightarrow \mu_j^{\alpha_{i'}} \neq \mu_j^{\alpha_i}\}. \tag{20}$$

For example, as shown in Fig. 5b, μ_4 only receives an assignment request from α_7, although it also falls within the coverage of α_{11}, since μ_2 has the largest scheduling weight of 4 for α_{11} and therefore the $\{\alpha_{11} \to \mu_4\}$ link of weight 3 is ignored. Similarly the $\{\alpha_6 \to \mu_6\}$ link of weight 4 is also a SSM, because the $\{\alpha_6 \to \mu_5\}$ and $\{\alpha_6 \to \mu_7\}$ links have a lower weight of 2. Hence, the AP-UE association after this initial selection is shown in Fig. 5b, where the low-weight links are only shown with dotted lines.

ii) *Tentative-cluster construction.* If a UE is offered multiple connection opportunities by different APs, this is said to be a Multiple-to-Single Matching (MSM), which may be defined as

$$\mathcal{M}_{\mathrm{MSM}} = \{(\alpha_i, \alpha_{i'}, \alpha_{i''}, \cdots) \to \mu_j^{\alpha_i} : \mu_j^{\alpha_i} = \mu_j^{\alpha_{i'}} = \mu_j^{\alpha_{i''}} = \cdots\}, \tag{21}$$

where we have $\mathcal{M}_{\mathrm{MSM}} = \{(\alpha_{10}, \alpha_{11}) \to \mu_2\}$ in the example of Fig. 5b, since μ_2 has the highest priority for both α_{10} and α_{11}. Furthermore, each MSM is assumed to construct a *tentative-cluster*, as also shown in Fig. 5b, where the shaded triangles indicate the hitherto unsupported UEs.

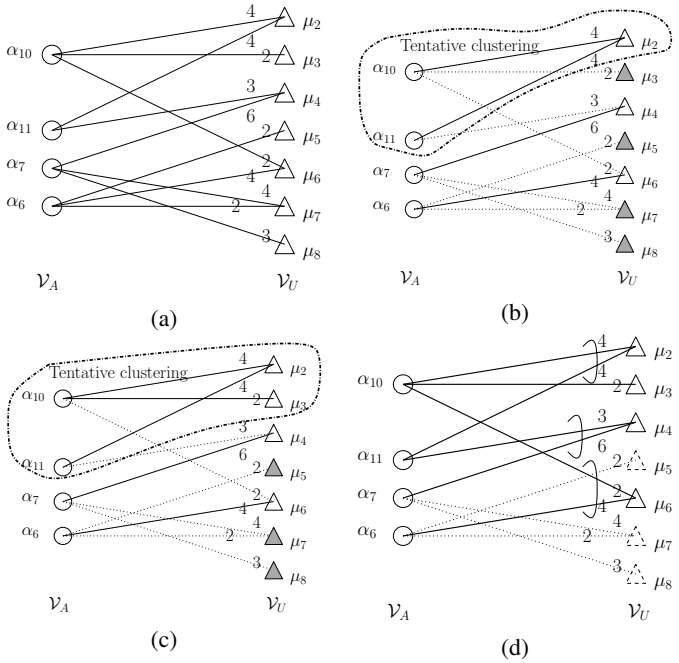

Fig. 5: (a) The network component considered. (b) Initial selection and tentative-cluster construction. The shaded triangles indicate the hitherto unsupported UEs. (c) Expansion of the tentative-cluster. (d) UC-VT cluster formation, where the incomplete ellipsoids indicate the specific UC-VT cooperation requests of the UEs and the finally unscheduled UEs are denoted by the triangles with dashed boundary.

iii) *Expansion of the tentative-cluster.* Within a tentative-cluster $(\alpha_i, \alpha_{i'}, \alpha_{i''}, \cdots) \rightarrow \mu_j^{\alpha_i}$, each AP α_i reselects a hitherto unsupported UE to be supported with the highest priority, provided that there are still unsupported UEs in $\mathcal{V}_{U,\alpha_i}$. Accordingly, as indicated by Fig. 5c, α_{10} reselects the unsupported UE μ_3, since the set $\mathcal{V}_U^{\alpha_{10}} \setminus (\mu_2, \mu_6) = \mu_3$ is non-empty and μ_3 is the only unsupported UE within the coverage of α_{10}. However, since the set $\mathcal{V}_U^{\alpha_{11}} \setminus (\mu_2, \mu_4) = \emptyset$ is empty, α_{11} does not have any additional UE to support.

iv) *Cluster formation.* In order to mitigate the inter-cluster interference, the scheduled UEs found in the overlapping areas of some neighbouring APs determine the cooperation of these APs. More explicitly, if a particular scheduled UE has the benefit of a LOS ray from several different APs, then the UE sends a cooperation request to these APs. For example, in Fig. 5d μ_2 sends its cooperation request to $\{\alpha_{10}, \alpha_{11}\}$, while μ_4 and μ_6 request cooperation with $\{\alpha_{11}, \alpha_7\}$ and $\{\alpha_{10}, \alpha_6\}$, respectively, as indicated by the incomplete ellipsoids. Thus all the cooperating APs and their matching UEs construct a single UC-VT cluster in the examples of Fig. 1b.

Recall that N_A APs are only capable of simultaneously supporting at most the same number of UEs according to (14). Therefore, during the expansion of the tentative-cluster, the number of active UEs becomes $(N_A + 1)$, provided that all APs can connect with an idle UE. Hence, the UE having the smallest priority is removed. Let us now provide an overview of the greedy cluster formation/MUS technique in form of Algorithm 21.

Algorithm 1: Proposed cluster formation/MUS Algorithm

```
Input: V_A, V_U;
for each time slot do
    Update: {P_{α_i} : α_i ∈ V_A};
    Initial selection:
    for each VLC AP α_i ∈ V_A do
        select μ_j^{α_i} = arg max_{μ_j ∈ V_{U,α_i}} (P_{α_i});
    end
    Tentative-cluster construction:
    if M_MSM ≠ ∅ then
        construct tentative-clusters;
    end
    Tentative-cluster expansion:
    for each tentative-cluster do
        for each AP α_i ∈ tentative-cluster do
            select the idle UE with the largest priority
            from V_{U,α_i};
        end
    end
    Cluster formation:
    Establish cooperation and construct UC-VT cluster
    formation;
    Vectored transmission and resource allocation;
end
```

TABLE II: Simulation Parameters

Transmitted optical power per LED lamp (P_t): 20×20 LEDs with 50mW per LED	20 [W]
Half of the receiver's FOV (ψ_F)	55°/57.5°/60°/62.5°
Reflectance factor (ρ)	0.8
Power of circled-LED lamp: 17×17 LEDs with 50mW per LED	14.4 [W]
Power of cornered-LED lamp: 23×32 LEDs with 50mW per LED	36.8 [W]

IV. Performance Evaluation

In this section, we will present our simulation results characterising the MUS and cluster formation algorithms, with a special emphasis on our UC-VT cluster formation. A 15m×15m×3m room model is considered, which is covered by a VLC down-link including (4×4) uniformly distributed optical APs at a height of 2.5m. The parameters of the LED arrays are summarized in TABLE II. Our investigations include both the LOS and the first reflected light-path, where the channel's DC attenuation is given by (1) and (2), respectively. Furthermore, as mentioned in Section II, ACO-OFDM is considered and the associated capacity is given as $R = \frac{B}{4}\log_2(1+\xi)$ according to [9], where ξ is the SINR of (8). Our simulation results were averaged over 50 independent snapshots and each snapshot is constituted by 50 consecutive time slots having a length of 1ms. The UEs at a height of 2.5m are random uniformly distributed at the beginning of each snapshot and they move randomly during the consecutive 50 time slots at a speed of 1m/s. The locations of the UEs are reported every time slot, i.e. every 1ms.

A. Complexity Analysis

As shown in Fig. 6a, when the number of UEs is less than 5, the exhaustive search may be an appealing low-complexity approach of finding the optimal solution for our joint optimization problem. However, the number of possible cluster formations found by employing the exhaustive search may become excessive with the number of UEs increased. Even if there are only 16 UEs supported by 16 APs, the average number of possible formations becomes as high as 5×10^6 in a single simulation run. By contrast, the complexity of the KM-algorithm based approach may become inadequate in low-UE-density scenarios. However, when the number of UEs is higher than that of the APs, the complexity is only linearly increased with the number of UEs, according to [26]. Fig. 6b shows both the normalized throughput and the sum utility of various cluster/cell formations, where the traditional NC cell formation designs relying on UFR and on the FR factor of two (FR-2) are considered as our benchmarkers. We adopt the MUS algorithm for the UFR and FR-2 discussed in our previous work [15]. Both the highest throughput attained and the sum utility are quantified for the proposed UC-VT cluster formation, whose optimal solution is found by the exhaustive search. The optimal MWM provides a similar solution as our proposed greedy algorithm, both of which are

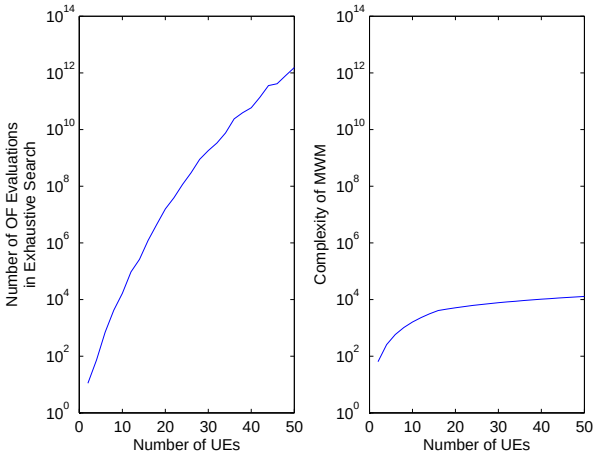

(a)

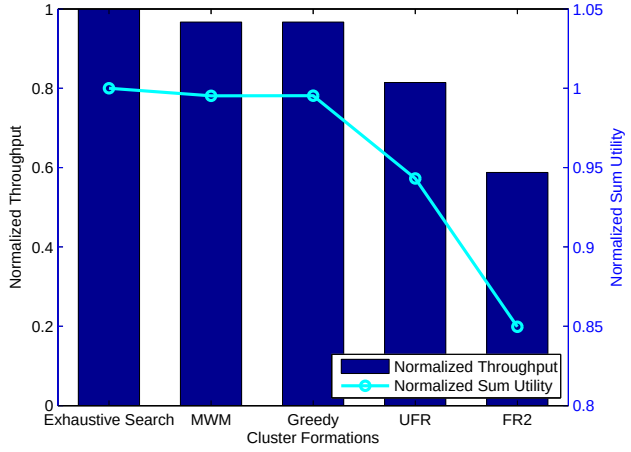

(b)

Fig. 6: (a) The complexity of the exhaustive search for finding the optimal UC-VT cluster formations and the complexity of KM-algorithm based MWM for finding a suboptimal cluster formation solution; (b) The normalized throughput and the normalized sum utility/OF value, where FOV = 110° and 10 UEs are assumed moving randomly at a speed of 1m/s.

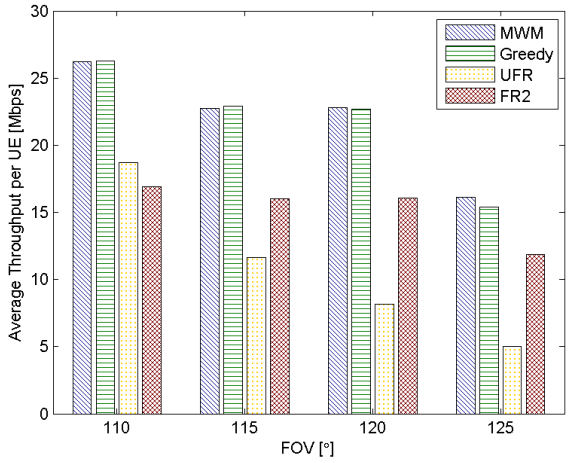

(a)

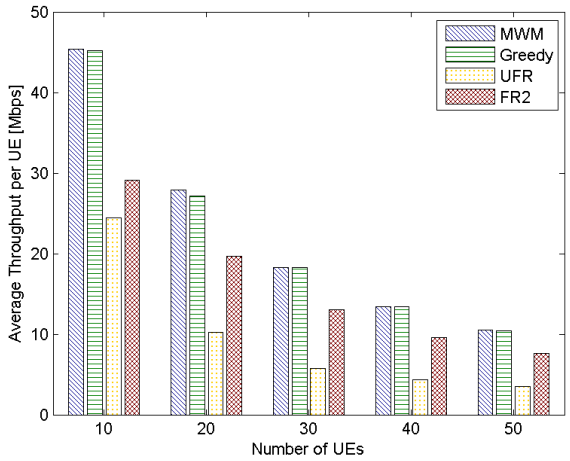

(b)

Fig. 7: (a) Average throughput per UE provided by different cluster formation/cell formation schemes for various FOVs and for 25 UEs. (b) Average throughput per UE provided by different cluster formation/cell formation schemes for various UE densities, where the FOV is 120° and the number of UEs is 25.

about 90% of the optimal exhaustive search-based value in the scenario considered. Therefore, we will omit the optimal exhaustive search in the rest of this treatise and we opt for the MWM solution as well as for the more practical greedy algorithm for finding the UC-VT cluster formation solution.

B. Throughput Investigations

1) Throughput Investigations for Various FOV and UE Density: Since the FOV is an influential parameter in VLC networks in Fig. 7a, we consider its effect on the system's performance. The average throughput per UE is reduced, when the FOV [3] is increased, due to the increased interference, while our proposed UC-VT cluster formation remains superior in all scenarios considered. In particular, observe in Fig. 7a that the UFR design exhibits the worst interference immunity and offers the lowest throughput, when the FOV is higher than 115°. Fig. 7b shows the average throughput per UE provided by different cluster formation/cell formation schemes associated with various UE densities, where the FOV is 120°. As expected, our proposed UC-VT cluster formation is capable of providing the highest average throughput for all the UE

[3]In order to evaluate the system's performance for various FOVs, we selected 110°/115° and 120°/125°. In the former scenario, the UE is capable of receiving data from two neighboring APs and the area contaminated by potential interference is modest. When the FOV is increased to 120°/125°, the UE is capable of receiving data from four APs and the potential interference-contaminated area is also increased. These four FOVs correspond to different interference levels, although their absolute values are quite similar.

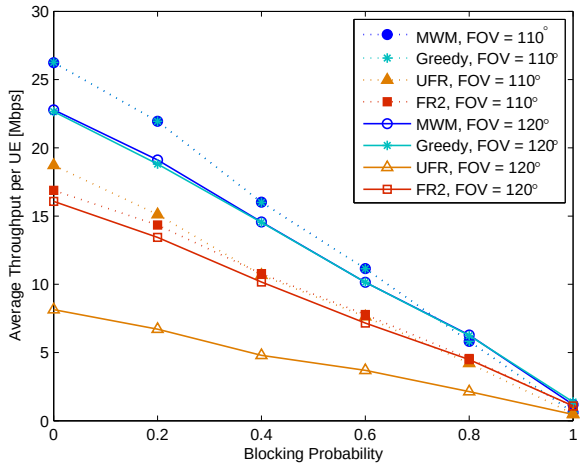

Fig. 8: Average UE throughput of our VLC system for various blocking probabilities and FOVs supporting 25 UEs in each scenario.

densities considered.

2) Throughput Investigations for Various LOS Blocking Probabilities: As mentioned in Section I, the performance of VLC systems is expected to be seriously degraded in non-LOS scenarios. In order to investigate the non-LOS behaviour of this VLC system, we introduce the LOS blocking probability P_b and assume that the achievable data rate $\tilde{R}$ obeys a Bernoulli distribution [13], with the probability mass function of:

$$f(\tilde{R}) = \begin{cases} 1 - P_b, & \text{if} \quad \tilde{R} = R_s, \\ P_b, & \text{if} \quad \tilde{R} = R_r, \end{cases} \tag{22}$$

where R_s and R_r denote the achievable data rate of the UE either in the presence or absence of LOS reception. Then the VLC down-link data rate may be written as $\tilde{R} = P_b \cdot R_r + (1 - P_b) \cdot R_s$. At this stage, we assume that all LOS paths are blocked with an equal probability. As shown in Fig. 8, the average UE throughput attained is reduced upon increasing the LOS blocking probability in all the scenarios considered, but our UC-VT cluster formation still achieves a higher throughput. Furthermore, the system performance of the MWM approach and of our proposed greedy cluster formation/MUS algorithm remains quite similar, regardless of the specific blocking probability and FOV.

C. Fairness Investigations

In order to investigate the grade of fairness experienced by the UEs, the Service Fairness Index (SFI) of [31] is introduced. The objective of ensuring fairness amongst the UEs is to guarantee that all UEs benefit from the same throughput within a given period, provided that the UEs' data rate requirements are identical [12], which is often unrealistic. The SFI was defined as [31]:

$$\text{SFI} = \frac{\max |\tilde{R}_{\mu_j} - \tilde{R}_{\mu_{j'}}|}{\sum_j \tilde{R}_{\mu_j} / N_U}, \tag{23}$$

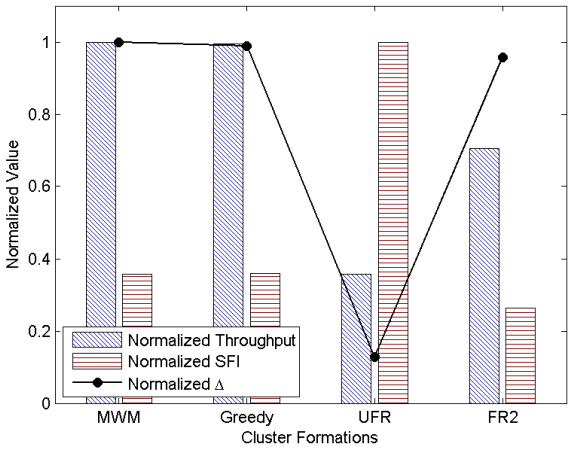

(a)

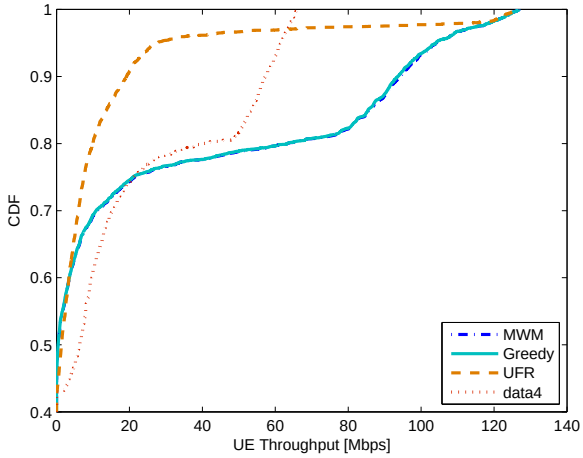

(b)

Fig. 9: (a) The normalized average throughput and the Service Fairness Index (SFI) of various cluster formation/cell formation schemes; (b) CDF of the UE throughput, where the number of UEs is 25 and we have FOV = 120°.

which reflects the maximum throughput-difference of different UEs. If the SFI is low, the throughput-difference is low and the UEs are served fairly, while if the SFI is high, the UEs experiencing a lower data rate may complain about their unfair treatment. Furthermore, by jointly considering the throughput, we may define

$$\Delta = \frac{\text{Average throughput per UE}}{\text{SFI}}. \tag{24}$$

Hence, Δ constitutes a comprehensive system performance metric, joint characterising both the throughput as well as the service fairness. If Δ is low, the system either provides a low throughput or a poor fairness; and vice versa. Fig. 9a shows the normalized throughput and SFI of various cell formations and cluster formations, where the UFR design has the worst performance associated with the lowest Δ. Moreover, the Cumulative Distribution Function (CDF) of the UE throughput is shown in Fig. 9b. It can be seen that the UE may have as

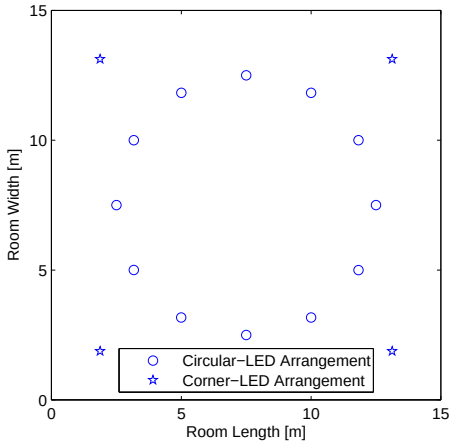

(a)

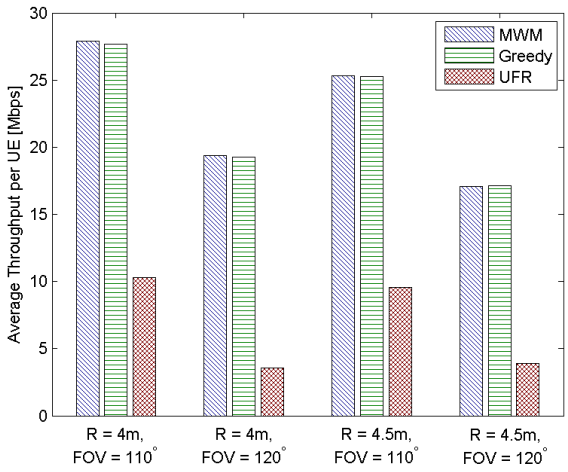

(b)

Fig. 10: (a) shows the LED-arrangement, where the LED circle has a radius of 4.5m and the corner LEDs are at 1.875m from the walls. (b) System performance of the LED arrangement seen in (a) for 25 UEs.

high as 40% probability of remaining unserved during each time slot in all the scenarios considered.

D. Irregular VLC AP Arrangements

Our proposed UC-VT cluster formation and MUS scheme may be readily applied to arbitrary topologies. Let us consider Fig. 10a, for example. This specific VLC AP arrangement was advocated in [32] for reducing the Signal-to-Noise-Ratio (SNR) fluctuation and was also employed in [16] for implementing a scheduling algorithm. As shown in Fig. 10a, 12 LED lamps constitute a circle and 4 LED lamps are placed in the corners at a height of 2.5m, which are referred to here as the circular-LED arrangement and corner-LED arrangement, respectively. The power of each LED array is 14.4W and 36.8W in the circular- and corner-arrangements of our simulations. Thus the total number of optical APs remains 16 and the sum of their transmission power is at most 320W, which is the same as that of the regular (4×4) LED array arrangement. Fig. 10b shows the average throughput per UE for the LED arrangement of Fig. 10a. The average throughput is slightly reduced, when the radius of the LED circle is increased from 4m to 4.5m, but our proposed UC-VT cluster formation still outperforms the traditional cell formation design in all scenarios of this circular LED arrangement.

V. Conclusions

In this paper, an amorphous UC-VT cluster formation was proposed for mitigating the ICI and to allow a single cluster to support multiple UEs. The MUS problem combined with our UC-VT cluster formation was investigated and the optimal solution was found by an exhaustive search approach. Since the exhaustive search may become complex, the original joint problem was reformulated as a MWM problem, which was solved by the classic KM-algorithm-based method. In order to further reduce the computational complexity, an efficient greedy MUS algorithm was proposed for constructing our UC-VT clusters. Our simulation results demonstrated that the UC-VT cluster formation is capable of providing a higher average UE throughput than the traditional NC cell designs in all the scenarios considered. Despite the promise of the UC-VT cluster formation, naturally, some challenges arise when incorporating our system-level UC design into VLC environments. The open challenges may be highlighted from various perspectives, including the acquisition of accurate location information, the research of robustness to LOS blocking, the technology counterpart to be used for up-link support, etc.

Appendix A
KM-algorithm-based Approach for Finding the Optimal MWM

Let us first rely on Lemma 1, where having independent elements indicates that none of them occupies the same row or column.

Lemma 1. *(König Theorem) [26]. If z is the maximum number of independent zero elements in the matrix (a_{α_i,μ_j}), then there are z lines (rows, columns or both) containing all the zeros elements of (a_{α_i,μ_j}).*

First, the weight matrix $(\omega_d(e_{\alpha_i,\mu_j}))$ of Fig. 3a is formulated, as shown in Fig. 11a, where the weight is set to zero when there is no link between two vertices. Our problem is that of maximizing the sum weight, while the KM algorithm is suitable for a minimization problem. We have to construct an equivalent matrix (a_{α_i,μ_j}) for $(\omega_d(e_{\alpha_i,\mu_j}))$, according to Theorem 1. The maximum element $(\omega_d(e_{\alpha_i,\mu_j}))$ is selected and forms (c_{α_i}), where we have $(c_{\alpha_i}) = [4,4,6,4]^{\mathrm{T}}$ in our example. Let $(c_{\alpha_i} - \omega_d(e_{\alpha_i,\mu_j}))$ be the matrix (a_{α_i,μ_j}), as shown in Fig. 11b, and its optimal matching solution minimizing the sum weight is also optimal for our MWM problem. Next, find a zero in each column of $(c_{\alpha_i} - \omega_d(e_{\alpha_i,\mu_j}))$. If however there is no starred zero either in its row or in its column, we mark it by a star, again as shown in Fig. 11b. Then we mark every column containing a 0^* by a vertical line and all the 0^* form a set of independent zeros, since none of them occupies the

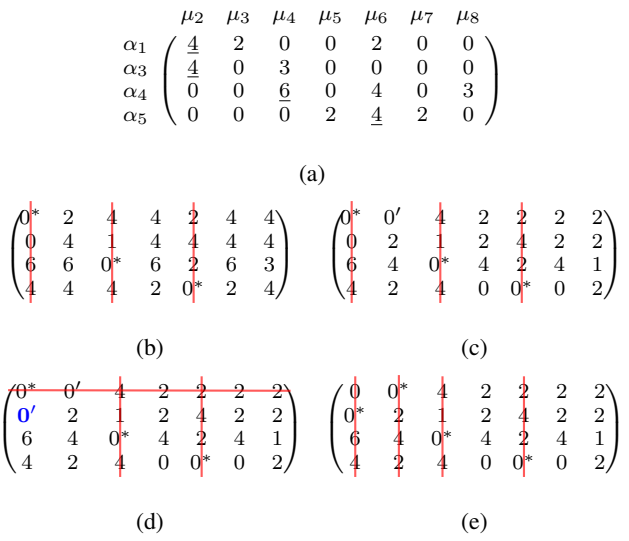

Fig. 11: (a) The weight matrix $(\omega_d(e_{\alpha_i,\mu_j}))$ of $\mathcal{Q}_2$, where the maximum element of each row is underlined. (b) Initialization step. The equivalent matrix (a_{α_i,μ_j}) of $(\omega_d(e_{\alpha_i,\mu_j}))$ is obtained as $(a_{\alpha_i,\mu_j}) = (c_{\alpha_i} - \omega_d(e_{\alpha_i,\mu_j}))$, where we have $(c_{\alpha_i}) = [4,4,6,4]^{\mathrm{T}}$. Find and mark the zero by a star, if there are no starred zeros in its row or in its column. Cover every column containing a 0^* by a vertical line. (c) Adjustment step. (a_{α_i,μ_j}) is modified as $(a_{\alpha_i,\mu_j} - c_{\alpha_i} + r_{\mu_j})$, where $(c_{\alpha_i}) = [0,0,0,0]^{\mathrm{T}}$ and $(r_{\mu_j}) = [0,-2,0,-2,0,-2,-2]$. Mark the uncovered zeros by the upper prime. (d) Explicitly, if there is a starred zero in the primed zero's row, mark this row by a line and remove the vertical line for the column of the starred zero. (e) Starred zero and primed zero alternating. Remove all lines. Recover the columns containing 0^*. Optimal solution found.

same row or column. The above-mentioned procedure is our initialization step, which may be described as:

i) *Initialization.* Generate an initial label set (c_{α_i}), where for each row α_i we have:

$$c_{\alpha_i} = \max_{\mu_j}(\omega_d(e_{\alpha_i,\mu_j})), \qquad \mu_j = 1,\cdots,N_{U,\mathcal{Q}_m}. \tag{25}$$

Thus, the equivalent matrix is constructed as $(c_{\alpha_i} - \omega_d(e_{\alpha_i,\mu_j}))$. Generate an initial matching $\mathcal{M}_{\mathcal{Q}_m}$ by finding and marking independent zeros denoted by $z_j^{(\alpha_i,\mu_j)}$ using a star, whose superscript corresponds to its index in $(c_{\alpha_i} - \omega_d(e_{\alpha_i,\mu_j}))$, where we have:

$$\begin{aligned} &\forall z_j^{(\alpha_i,\mu_j)} \in (z_j), \quad z_{j'\neq j}^{(\alpha_i'\neq\alpha_i,\mu_j)} \notin (z_j), \\ &\forall z_j^{(\alpha_i,\mu_j)} \in (z_j), \quad z_{j'\neq j}^{(\alpha_i,p_{\alpha_i'}\neq\mu_j)} \notin (z_j). \end{aligned} \tag{26}$$

If $|(z_j)| = \min\{N_{A,\mathcal{Q}_m}, N_{U,\mathcal{Q}_m}\}$ columns are marked, we find the desired matching, where each AP matches a specific UE and the sum weight of their links is maximized, which furthermore form a UC-VT cluster. Otherwise, the cardinality of the matching will be iteratively increased during the following steps.

If there are no unmarked zeros as shown in Fig. 11b, the current matrix should be modified according to Theorem 1, which leads to the following adjustment step.

ii) *Adjustment.* Let h be the smallest unmarked element of the matrix and construct a column vector (c_{α_i}) and a row vector (r_{μ_j}) by the following rules: if the α_ith row is covered, $c_{\alpha_i} = h$; otherwise, $c_{\alpha_i} = 0$. If the μ_jth column is covered, $r_{\mu_j} = 0$; otherwise, $r_{\mu_j} = -h$. In our example, (a_{α_i,μ_j}) is updated as $(a_{\alpha_i,\mu_j} - c_{\alpha_i} + r_{\mu_j})$ and $(c_{\alpha_i}) = [0,0,0,0]^{\mathrm{T}}$ and $(r_{p_i}) = [0,-2,0,-2,0,-2,-2]$, as shown in Fig. 11c.

Then let us choose and mark an unmarked zero by priming it. If there is a starred zero in its row, mark this row by a line and remove the line from the column of the starred zero, as shown in Fig. 11d. Then we prime another unmarked zero in the second row indicated by the bold font, but there is no starred zero in its row. According to the starred and primed zero alternating rules of [26], we obtain the matrix seen in Fig. 11e, where the number of independent zeros reached its maximum given by the number of rows. Correspondingly, the number of lines containing all these zeros becomes maximal, as stated by Lemma 1, where the maximum number of independent zeros is equal to the number of lines containing them. The algorithm terminates here in our scenario. However, if the number of marked columns is still insufficient, the set of independent zeros has to be increased by iteratively repeating the above-mentioned steps, commencing from the Adjustment stage. Thus, we find the optimal solution for our MWM, which is $\{\alpha_{10} \to \mu_3, \alpha_{11} \to \mu_2, \alpha_7 \to \mu_4, \alpha_6 \to \mu_6\}$, namely the same as indicated in Fig. 3b.

REFERENCES

[1] L. Hanzo, H. Haas, S. Imre, D. O'Brien, M. Rupp, and L. Gyongyosi, "Wireless myths, realities, and futures: From 3G/4G to optical and quantum wireless," in *Proceedings of the IEEE*, vol. 100, May 2012, pp. 1853–1888.

[2] D. O'Brien, H. Haas, S. Rajbhandari, H. Chun, G. Faulkner, K. Cameron, A. V. Jalajakumari, R. Henderson, D. Tsonev, M. Ijaz *et al.*, "Integrated multiple-input multiple-output visible light communications systems: recent progress and results," in *SPIE OPTO*, 2015, pp. 93 870P–93 870P.

[3] D. Tsonev, S. Videv, and H. Haas, "Towards a 100 Gb/s visible light wireless access network," *Optics Express*, vol. 23, no. 2, pp. 1627–1637, Jan 2015.

[4] D. Tsonev, H. Chun, S. Rajbhandari, J. McKendry, S. Videv, E. Gu, M. Haji, S. Watson, A. Kelly, G. Faulkner, M. Dawson, H. Haas, and D. O'Brien, "A 3-Gb/s single-LED OFDM-based wireless VLC link using a gallium nitride μLED," *IEEE Photonics Technology Letters*, vol. 26, no. 7, pp. 637–640, April 2014.

[5] S. Dissanayake and J. Armstrong, "Comparison of ACO-OFDM, DCO-OFDM and ADO-OFDM in IM/DD systems," *Journal of Lightwave Technology*, vol. 31, no. 7, pp. 1063–1072, Apr. 2013.

[6] A. Azhar, T. Tran, and D. O'Brien, "A Gigabit/s indoor wireless transmission using MIMO-OFDM visible-light communications," *IEEE Photonics Technology Letters*, vol. 25, no. 2, pp. 171–174, Jan 2013.

[7] J. Grubor, S. Randel, K.-D. Langer, and J. Walewski, "Broadband information broadcasting using LED-based interior lighting," *Journal of Lightwave Technology*, vol. 26, no. 24, pp. 3883–3892, Dec. 2008.

[8] J. Armstrong and B. Schmidt, "Comparison of asymmetrically clipped optical OFDM and DC-biased optical OFDM in AWGN," *Communications Letters, IEEE*, vol. 12, no. 5, pp. 343–345, May 2008.

[9] X. Li, R. Mardling, and J. Armstrong, "Channel capacity of IM/DD optical communication systems and of ACO-OFDM," in *IEEE ICC 2007*, June 2007, pp. 2128–2133.

[10] T. Komine and M. Nakagawa, "Fundamental analysis for visible-light communication system using LED lights," *IEEE Transactions on Consumer Electronics*, vol. 50, no. 1, pp. 100–107, Feb. 2004.

[11] "IEEE standard for local and metropolitan area networks–part 15.7: Short-range wireless optical communication using visible light," *IEEE Std 802.15.7-2011*, pp. 1–309, Sep. 2011.

[12] X. Li, R. Zhang, and L. Hanzo, "Cooperative load balancing in hybrid visible light communications and WiFi," *IEEE Transactions on Communications*, vol. PP, no. 99, pp. 1–1, Mar. 2015.

[13] F. Jin, R. Zhang, and L. Hanzo, "Resource allocation under delay-guarantee constraints for heterogeneous visible-light and RF femtocell," *IEEE Transactions on Wireless Communications*, vol. 14, no. 2, pp. 1020–1034, Feb 2015.

[14] C. Chen, N. Serafimovski, and H. Haas, "Fractional frequency reuse in optical wireless cellular networks," in *IEEE PIMRC 2013*, Sep. 2013, pp. 3594–3598.

[15] X. Li, R. Zhang, J. Wang, and L. Hanzo, "Cell-Centric and User-Centric Multi-User scheduling in visible light communication aided networks," in *IEEE ICC 2015 (06) ONS*, Jun. 2015.

[16] Y. Tao, X. Liang, J. Wang, and C. Zhao, "Scheduling for indoor visible light communication based on graph theory," *Optics Express*, vol. 23, no. 3, pp. 2737–2752, Feb 2015.

[17] R. Zhang, J. Wang, Z. Wang, Z. Xu, C. Zhao, and L. Hanzo, "Visible light communications in heterogeneous networks: Paving the way for user-centric design," *IEEE Wireless Communications*, vol. 22, no. 2, pp. 8–16, April 2015.

[18] D. Bykhovsky and S. Arnon, "Multiple access resource allocation in visible light communication systems," *Journal of Lightwave Technology*, vol. 32, no. 8, pp. 1594–1600, April 2014.

[19] M. Biagi, S. Pergoloni, and A. Vegni, "Last: a framework to localize, access, schedule and transmit in indoor VLC systems," *Journal of Lightwave Technology*, vol. PP, no. 99, pp. 1–1, 2015.

[20] X. Huang, X. Fu, and W. Xu, "Incremental scheduling scheme for indoor visible light communication," *Electronics Letters*, vol. 51, no. 3, pp. 268–270, Feb 2015.

[21] O. Babatundi, L. Qian, and J. Cheng, "Downlink scheduling in visible light communications," in *WCSP 2014*, Oct 2014, pp. 1–6.

[22] H. Kushner and P. Whiting, "Convergence of proportional-fair sharing algorithms under general conditions," *IEEE Transactions on Wireless Communications*, vol. 3, no. 4, pp. 1250–1259, July 2004.

[23] J. Akhtman and L. Hanzo, "Power versus bandwidth-efficiency in wireless communications: The economic perspective," in *IEEE VTC 2009*, Sep. 2009, pp. 1–5.

[24] H. W. Kuhn, "The Hungarian method for the assignment problem," *Naval research logistics quarterly*, vol. 2, no. 1-2, pp. 83–97, Mar. 1955.

[25] J. Munkres, "Algorithms for the assignment and transportation problems," *Journal of the Society for Industrial & Applied Mathematics*, vol. 5, no. 1, pp. 32–38, Mar. 1957.

[26] F. Bourgeois and J.-C. Lassalle, "An extension of the Munkres algorithm for the assignment problem to rectangular matrices," *Communications of the ACM*, vol. 14, no. 12, pp. 802–804, Dec. 1971.

[27] M. M. Halldórsson and J. Radhakrishnan, "Greed is good: Approximating independent sets in sparse and bounded-degree graphs," *Algorithmica*, vol. 18, no. 1, pp. 145–163, May 1997.

[28] K. Zheng, F. Liu, Q. Zheng, W. Xiang, and W. Wang, "A graph-based cooperative scheduling scheme for vehicular networks," *IEEE Transactions on Vehicular Technology*, vol. 62, no. 4, pp. 1450–1458, May 2013.

[29] J. Kahn and J. Barry, "Wireless infrared communications," in *Proceedings of the IEEE*, vol. 85, no. 2, Feb. 1997, pp. 265–298.

[30] T. Bu, L. Li, and R. Ramjee, "Generalized proportional fair scheduling in third generation wireless data networks," in *Proceedings of INFOCOM 2006*, Apr. 2006, pp. 1–12.

[31] B. Bensaou, D. H. K. Tsang, and K. T. Chan, "Credit-based fair queueing (CBFQ): a simple service-scheduling algorithm for packet-switched networks," *IEEE/ACM Transactions on Networking*, vol. 9, no. 5, pp. 591–604, Oct. 2001.

[32] Z. Wang, C. Yu, W.-D. Zhong, J. Chen, and W. Chen, "Performance of a novel LED lamp arrangement to reduce SNR fluctuation for multi-user visible light communication systems," *Optics Express*, vol. 20, no. 4, pp. 4564–4573, Feb 2012.

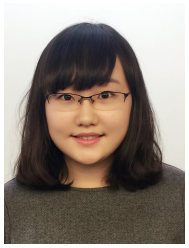

Xuan Li received her B.Eng. degree (June 12) in Optical Information Science and Technology from Beijing Institute of Technology, China. She is currently working towards the PhD degree with the Southampton Wireless Group, University of Southampton, UK. Her research interests include visible light communications, heterogeneous networks, resource allocation and scheduling algorithms.

Fan Jin received his PhD (Jun 15) from Southampton University, UK and his BSc (Jun 10) from Huazhong University of Science and Technology(HUST), China. He is now working as an engineer in Huawei, China. He has received a scholarship under the UK-China Scholarships for Excellence Programme. His research interests include multi-user communications, radio resource allocation, spectrum sensing and interference management in femtocells and heterogeneous networks.

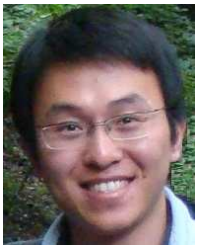

Rong Zhang (M'09) received his PhD (Jun 09) from Southampton University, UK and his BSc (Jun 03) from Southeast University, China. Before doctorate, he was an engineer (Aug 03-July 04) at China Telecom and a research assistant (Jan 06-May 09) at Mobile Virtual Center of Excellence (MVCE), UK. After being a post-doctoral researcher (Aug 09-July 12) at Southampton University, he took industrial consulting leave (Aug 12-Jan 13) for Huawei Sweden R& D as a system algorithms specialist. Since Feb 13, he has been appointed as a lecturer at CSPC group of ECS, Southampton University. He has 40+ journals in prestigious publication avenues (e.g. IEEE, OSA) and many more in major conference proceedings. He regularly serves as reviewer for IEEE transactions/journals and has been several times as TPC member/invited session chair of major conferences. He is the recipient of joint funding of MVCE and EPSRC and is also a visiting researcher under Worldwide University Network (WUN). More details can be found at http://www.ecs.soton.ac.uk/people/rz.

Jiaheng Wang (S08M10-SM14) received the B.E. and M.S. degrees from Southeast University, Nanjing, China, in 2001 and 2006, respectively, and the Ph.D. degree in electrical engineering from the Hong Kong University of Science and Technology, Kowloon, Hong Kong, in 2010. He is currently an Associate Professor with the National Mobile Communications Research Laboratory (NCRL), Southeast University. From 2010 to 2011, he was with the Signal Processing Laboratory, ACCESS Linnaeus Center, KTH Royal Institute of Technology, Stockholm, Sweden. He also held a visiting position at the Department of Computer and Information Science, University of Macau, Macau. His research interests mainly include optimization in signal processing, wireless communications, and networks. Dr. Wang serves as an Associate Editor for the IEEE Signal Processing Letters. He is a recipient of the Humboldt Fellowship for Experienced Researchers, and a recipient of the Best Paper Award in WCSP 2014.

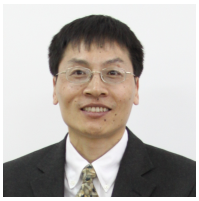

Zhengyuan Xu received his B.S. and M.S. degrees from Tsinghua University, Beijing, China, in 1989 and 1991, respectively, and Ph.D. degree from Stevens Institute of Technology, New Jersey, USA, in 1999. From 1991 to 1996, he was with Tsinghua Unisplendour Group Corporation, Tsinghua University, as system engineer and department manager. In 1999, he joined University of California, Riverside, first as Assistant Professor and then tenured Associate Professor and Professor. He was Founding Director of the multi-campus Center for Ubiquitous Communication by Light (UC-Light), University of California. In 2010, he was selected by the Thousand Talents Program of China, appointed as Professor at Tsinghua University, and then joined University of Science and Technology of China (USTC). He is Founding Director of the Optical Wireless Communication and Network Center, Founding Director of Wireless-Optical Communications Key Laboratory of Chinese Academy of Sciences, and Vice Dean of School of Information Science and Technology, in USTC. He is also a chief scientist of the National Key Basic Research Program (973 Program) of China. His research focuses on wireless communication and networking, optical wireless communications, geolocation, intelligent transportation, and signal processing. He has published over 200 journal and conference papers. He has served as an Associate Editor and Guest Editor for different IEEE and OSA journals. He was a Founding Chair of IEEE Workshop on Optical Wireless Communications.

Lajos Hanzo (http://www-mobile.ecs.soton.ac.uk) FREng, FIEEE, FIET, Fellow of EURASIP, DSc received his degree in electronics in 1976 and his doctorate in 1983. In 2009 he was awarded the honorary doctorate "Doctor Honoris Causa" by the Technical University of Budapest. During his 38-year career in telecommunications he has held various research and academic posts in Hungary, Germany and the UK. Since 1986 he has been with the School of Electronics and Computer Science, University of Southampton, UK, where he holds the chair in telecommunications. He has successfully supervised about 100 PhD students, co-authored 20 John Wiley/IEEE Press books on mobile radio communications totalling in excess of 10 000 pages, published 1400+ research entries at IEEE Xplore, acted both as TPC and General Chair of IEEE conferences, presented keynote lectures and has been awarded a number of distinctions. Currently he is directing a 100-strong academic research team, working on a range of research projects in the field of wireless multimedia communications sponsored by industry, the Engineering and Physical Sciences Research Council (EPSRC) UK, the European Research Council's Advanced Fellow Grant and the Royal Society's Wolfson Research Merit Award. He is an enthusiastic supporter of industrial and academic liaison and he offers a range of industrial courses. He is also a Governor of the IEEE VTS. During 2008 - 2012 he was the Editor-in-Chief of the IEEE Press and a Chaired Professor also at Tsinghua University, Beijing. His research is funded by the European Research Council's Senior Research Fellow Grant. For further information on research in progress and associated publications please refer to http://www-mobile.ecs.soton.ac.uk Lajos has 20 000+ citations.